

Journal Pre-proof

Dynamic coordination of miscible polymer blends towards highly designable shape memory effect

Xiaodong Wang, Haibao Lu, Xuqing Liu, Mokarram Hossain, Yong Qing Fu, Ben Bin Xu



PII: S0032-3861(20)30771-0

DOI: <https://doi.org/10.1016/j.polymer.2020.122946>

Reference: JPOL 122946

To appear in: *Polymer*

Received Date: 6 July 2020

Revised Date: 17 August 2020

Accepted Date: 19 August 2020

Please cite this article as: Wang X, Lu H, Liu X, Hossain M, Fu YQ, Xu BB, Dynamic coordination of miscible polymer blends towards highly designable shape memory effect, *Polymer*, <https://doi.org/10.1016/j.polymer.2020.122946>.

This is a PDF file of an article that has undergone enhancements after acceptance, such as the addition of a cover page and metadata, and formatting for readability, but it is not yet the definitive version of record. This version will undergo additional copyediting, typesetting and review before it is published in its final form, but we are providing this version to give early visibility of the article. Please note that, during the production process, errors may be discovered which could affect the content, and all legal disclaimers that apply to the journal pertain.

© 2020 Elsevier Ltd. All rights reserved.

Dynamic coordination of miscible polymer blends towards highly designable shape memory effect

Xiaodong Wang^a, Haibao Lu^{a,*}, Xuqing Liu^b, Mokarram Hossain^c, Yong Qing Fu^d and Ben Bin Xu^{d,*}

^aScience and Technology on Advanced Composites in Special Environments Laboratory, Harbin Institute of Technology, Harbin 150080, China

^bSchool of Materials, The University of Manchester, Oxford Road, M13 9PL, UK

^cZienkiewicz Centre for Computational Engineering, College of Engineering, Swansea University, Swansea, UK

^dFaculty of Engineering and Environment, Northumbria University, Newcastle upon Tyne, NE1 8ST, UK

*Corresponding author, E-mail addresses: luhb@hit.edu.cn and ben.xu@northumbria.ac.uk

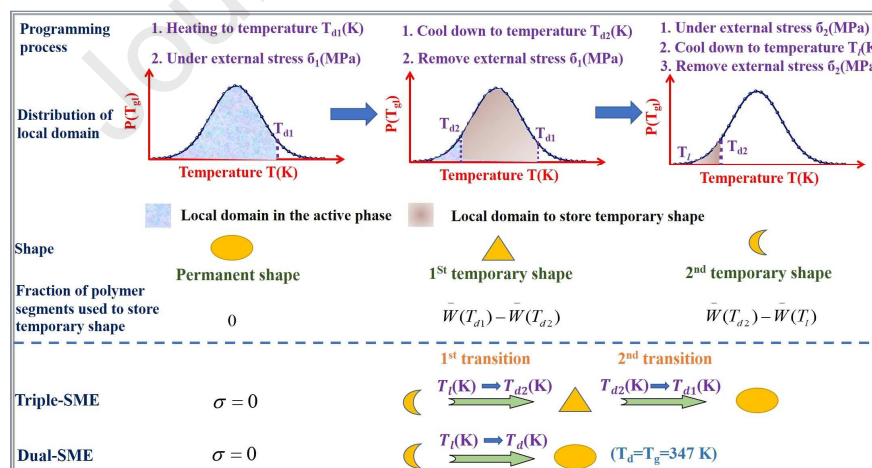


Illustration of mechanical processes and their working mechanisms of SME and TME in miscible polymer blends

Dynamic coordination of miscible polymer blends towards highly designable shape memory effect

Xiaodong Wang^a, Haibao Lu^{a,*}, Xuqing Liu^b, Mokarram Hossain^c, Yong Qing Fu^d and Ben Bin Xu^{d,*}

^aScience and Technology on Advanced Composites in Special Environments Laboratory, Harbin Institute of Technology, Harbin 150080, China

^bSchool of Materials, The University of Manchester, Oxford Road, M13 9PL, UK

^cZienkiewicz Centre for Computational Engineering, College of Engineering, Swansea University, Swansea, UK

^dFaculty of Engineering and Environment, Northumbria University, Newcastle upon Tyne, NE1 8ST, UK

*Corresponding author, E-mail addresses: luhb@hit.edu.cn and ben.xu@northumbria.ac.uk

ABSTRACT: Miscible polymer blends offer great designability on shape memory effect (SME) with adjustable mechanical properties and stimuli-responsiveness, by simply changing the constituent compositions. However, the thermodynamics understanding behind those SMEs on miscible polymer blends are yet to be explored. This paper describes an approach to achieve highly designable SMEs with adjustable glass transition temperature (T_g) and width of glass transition zone by dynamically coordinating components in miscible blends. An extended domain size model was formulated based on the Adam-Gibbs theory and Gaussian distribution theory to study the synergistic coordination of component heterogeneities on conformational entropy,

glass transition and relaxation behaviour of the miscible blend. The effectiveness of model was demonstrated by applying it to predict dual- and triple-SMEs in miscible polymer blends, where the theoretical results show good agreements with the experiment results. We expect this study provide an effective guidance on designing advanced miscible polymer blends based on the SME.

Keywords: Miscible polymer blends; shape memory effect; dynamic coordination

1. Introduction

Shape memory effect (SME) based structural morphing process is usually considered as reversibly switching of conformational entropy between thermodynamic meta-states in polymers, which could be directly triggered by heat, solvent, light or electric field [1-4]. SME is of great scientific interests because its working principles are linked closely with both macromolecule thermodynamics and macroscopic polymer properties [5], thus leading to smart transition to regain their permanent shape from a temporary one at the presence of external stimuli. These so-called shape memory polymers (SMPs) have emerging applications in biomedical devices [6,7], deployable structures [8,9], sensors and actuators [10].

Recent developments have renewed the capacity of SMP by memorizing two, three, and even four different shapes by designing various macromolecular compositions and architectures/networks [11,12]. Multiple-shape memory effect (multiple-SME) can be generated by introducing several different glassy

and/or melting components in the soft matrix [13,14], or recovering an additional shape upon experiencing an appropriate thermomechanical programming history for the polymer with broadened glass transition temperature zones [15,16]. The intermediate shapes can therefore be tuned by varying the input mechanical energy at each deformation temperature, and more interestingly the recovery of each temporary shape can be facilitated in vicinity of the corresponding initial deformation temperature, known as temperature memory effect (TME) [17].

Multiple-SME and TME have been realized in miscible polymer blends [18-20], where both their glass transition temperatures and widths are important properties to determine their shape recoveries. However, their working principles are not fully understood yet and physical modelling is a huge challenge. Recently, the linear phase transition theory [21] was developed to characterize the visco-elastic properties [22] and predict the rate-dependent shape memory behaviours of SMPs [23]. Meanwhile, the multibranch model [24,25] was introduced to replace the linear phase transition model [26] for quantitative analysis of viscoelasticity in SMPs. However, the modelling is mostly phenomenological and mainly determined by experiments.

In this paper, we describe a thermodynamics study based on Adam-Gibbs (AG) theory [27,28] and Gaussian distribution theory [29], to understand the broadened glass transition temperature range of miscible polymer blends with dynamic coordination of different phases. The dependences of conformational

entropy and relaxation behaviour on components' heterogeneities have been identified as the driving force for dynamic coordination in miscible polymer blends [29]. By combining the AG theory with coupling model [30], a kinetic model is established to study the viscoelastic behaviours of local transition domains. Then, a model of nonlinear phase transition probability is formulated to characterize the SME and TME as functions of temperature, relaxation time and deformation temperature. Finally, the newly proposed models are validated using the experimental results of the thermomechanical and free recovery behaviours of miscible polymer blends [18], and then accurately predicted their viscoelastic relaxation behaviours [18]. It should be noted that the theoretical model works in the regime of viscoelasticity, thus, plastic deformation and the dependence of the residual strain on programming temperature and deformation rate are not considered in the calculation.

2. Modelling on the glass transition in miscible polymer blends

Based on the AG theory [27,28], a coordinated domain relaxation model is generally introduced to characterize the phase transition of amorphous materials within glass transition temperature zone. The conformers in one domain are required to move cooperatively [28]. One disadvantage for AG theory is that it does not work well for more than two miscible components. However, the AG theory can be extended with Gaussian distribution theory [29] and coupling model [30] to capture the coordinated transition probability for miscible polymer blends with more than two miscible components.

Coordinated transition probability $W_0(T,t)$ of the conformers has a constitutive relationship with local activation energy of the domain, which can be written as [31]:

$$W_0(T,t) = 1 - [1 - \exp(-\Delta H(z) / (RT))]^\nu \quad (1)$$

where the frequency factor ν is assumed negligibly dependent on temperature, R is the gas constant ($R=8.314 \text{ J} / (\text{mol} * \text{K})$) and z is the domain size.

The key concept of the AG theory is that all the conformers in one domain must have the same activation energy and relax cooperatively, thus, the activation energy can be written as a function of domain size (z):

$$\Delta H(z) = z(T)\Delta\mu \quad (2)$$

where $\Delta\mu$ is the activation energy for conformer per mole.

The domain size ($z(T)$) can be derived from configurational entropy ($S_c(T)$) as [27]:

$$z(T) = \frac{s^*}{S_c(T)} = \frac{T(T^* - T_{0l})}{T^*(T - T_{0l})} \quad (3)$$

where T^* is the high temperature limit, where the conformers are sufficiently far apart that each can relax independently from the neighbors, and the configurational entropy ($S_c(T)$) achieves to the highest value of s^* [27]. On the other hand, parameter T_{0l} is the low temperature limit of the local domain where all conformers are moved cooperatively and the configurational energy ($S_c(T)$) is zero at this temperature.

The AG theory form of relaxation time can then be obtained [28]:

$$\tau(T) = \tau_0 \exp(z(T)\Delta\mu / (RT)) = \tau_0 \exp\left(\frac{\Delta\mu(T^* - T_{0l})}{RT^*(T - T_{0l})}\right) \quad (4)$$

By substituting equations (2) and (3) into (1), we can obtain the transition probability of local domain with the low-temperature limit (T_{0l}):

$$W_0(T, t, T_{0l}) = 1 - \left[1 - \exp\left(-\frac{\Delta\mu(T^* - T_{0l})}{RT^*(T - T_{0l})}\right)\right]^{vt} \quad (5)$$

However, the miscible polymer blends have a huge number of local domains with different sizes and each one has its own glass transition temperature. Here the coupling model is used to modify the AG theory to model the cooperative dynamics of these domains using a decay function ($\phi(t)$), which has the following form [32]:

$$\phi(t) = \exp\left\{-\left[t / \tau^*(T)\right]^\beta\right\} \quad (6)$$

where β is a constant ($0 \leq \beta \leq 1$), relaxation time ($\tau^*(T)$) can be written from equation (4):

$$\tau^*(T) = [B\tau(T)]^{1/\beta} = \left[B\tau_0 \exp\left(\frac{\Delta\mu(T^* - T_{0l})}{RT^*(T - T_{0l})}\right)\right]^{1/\beta} \quad (7)$$

where B is a fitting constant.

In combination of equations (6) and (7), the decay function of local domain as a function of T_{0l} can be written as:

$$\phi(t, T_{0l}) = \exp\left\{-\left[t / \left(B\tau_0 \exp\left(\frac{\Delta\mu(T^* - T_{0l})}{RT^*(T - T_{0l})}\right)\right)^{1/\beta}\right]^\beta\right\} \quad (8)$$

Substituting equation (8) into (5), the cooperative transition probability, $W(T, t)$, by considering both cooperative relaxation in one domain and interactive relationship among neighboring domains, can be written:

$$\begin{aligned}
W(T, t, T_{0l}) &= W_0(T, t, T_{0l}) [1 - \phi(t, T_{0l})] \\
&= \left\{ 1 - \left[1 - \exp \left(- \frac{\Delta\mu(T^* - T_{0l})}{RT^* (T - T_{0l})} \right) \right]^{v_l} \right\} \left\{ 1 - \exp \left\{ - \left[t / \left(B\tau_0 \exp \left(\frac{\Delta\mu(T^* - T_{0l})}{RT^* (T - T_{0l})} \right) \right)^{1/\beta} \right]^\beta \right\} \right\} \quad (9)
\end{aligned}$$

When the relaxation time $t \rightarrow \infty$, $\phi(t, T_{0l})$ is equal to zero, the transition behaviors of domains will be only determined by parameter T_{0l} . From the experimental data reported in Ref. [32], the difference between T_{0l} and glass transition temperature of local domain (T_{gl}) is a constant of ζ :

$$T_{gl} - T_{0l} = \zeta \quad (10)$$

By substituting equation (10) into (9), we can obtain the transition probability of local domain at temperature T and recovery time t :

$$\begin{aligned}
W(T, t, T_{gl}) &= \left\{ 1 - \left[1 - \exp \left(- \frac{\Delta\mu(T^* - T_{gl} + \zeta)}{RT^* (T - T_{gl} + \zeta)} \right) \right]^{v_l} \right\} \\
&\quad \left\{ 1 - \exp \left\{ - \left[t / \left(B\tau_0 \exp \left(\frac{\Delta\mu(T^* - T_{gl} + \zeta)}{RT^* (T - T_{gl} + \zeta)} \right) \right)^{1/\beta} \right]^\beta \right\} \right\} \quad (11)
\end{aligned}$$

The glass transition temperature of miscible polymer blends is determined by that of each component. In Ref. [29], glass transition temperature of local domain (T_{gl}) follows the form of Gaussian distribution, and writes:

$$P(T_{gl}) = \Phi_1 \frac{1}{\sqrt{2\pi w_1}} \exp \left\{ - \frac{(T_{gl} - T_{g1})^2}{2w_1} \right\} + (1 - \Phi_1) \frac{1}{\sqrt{2\pi w_2}} \exp \left\{ - \frac{(T_{gl} - T_{g2})^2}{2w_2} \right\} \quad (12)$$

where Φ is the content fraction, T_g is the glass transition temperature and w_i ($i=1, 2$) is the width of glass transition temperature zone of each component in the miscible polymer blends.

3. Theoretical model and experimental verification of SME in miscible polymer blends

According to equation (12), the distribution of local glass transition temperature results in the miscible polymer with a broadened width of glass transition temperature. Here the deformation temperature (T_d) is proposed to show the temperature for miscible polymer to be deformed at a relatively high temperature and then the deformation is kept by cooling the polymer back to a relative low temperature. In this process, the existence of deformation temperature (T_d) enables the mechanical energy stored in miscible polymer blends. As explained previously, both the SME and TME are originated from the release of stored mechanical energy [17,24]. Therefore, the phase evolution function (ϕ_f) equals to the fraction of the frozen volume in SMPs, e.g.:

$$\phi_f(T, t) = \frac{\varepsilon_s(T, t) - \varepsilon_r}{\varepsilon_{pre} - \varepsilon_r} \quad (13)$$

where ε_{pre} is the pre-loading strain, ε_s are the stored strain and ε_r is the residual strain when the phase transition is finished.

By integrating the domain with the local glass transition temperature (T_{gl}), we can obtain the phase transition probability ($\bar{W}(T, t)$):

$$\bar{W}(T, t) = \int_0^{+\infty} W(T, t, T_{gl}) P(T_{gl}) dT_{gl} = \int_0^{+\infty} W_0(T, t, T_{gl}) [1 - \phi(t, T_{gl})] P(T_{gl}) dT_{gl} \quad (14)$$

Then, the phase transition probability as a function of deformation temperature can be further written as:

$$\bar{W}(T_d) = \bar{W}(T = T_d, t = t_s) = \int_0^{+\infty} W_0(T_d, t_s, T_{gl}) [1 - \phi(t_s, T_{gl})] P(T_{gl}) dT_{gl} \quad (15)$$

where t_s is the loading time of miscible polymer by external stress.

The physical mechanism of SME and TME are illustrated in Figure 1. Initially, the miscible polymer blends are subjected to the first deformation temperature T_{d1} , and thus a certain fraction of component ($\bar{W}(T_{d1})$) is induced into its active state. Consequently, the miscible polymer blends are deformed at an external stress (σ_1) and then cooled down to a moderate temperature T_{d2} . Here the volume fraction of the active phase is $\bar{W}(T_{d2})$. $\bar{W}(T_{d1}) - \bar{W}(T_{d2})$ is used to store the 1st temporary shape. $\bar{W}(T_{d2})$ is used to store the 2nd temporary shape. The stored mechanical energy has been identified as the physical mechanism of SME and TME [17].

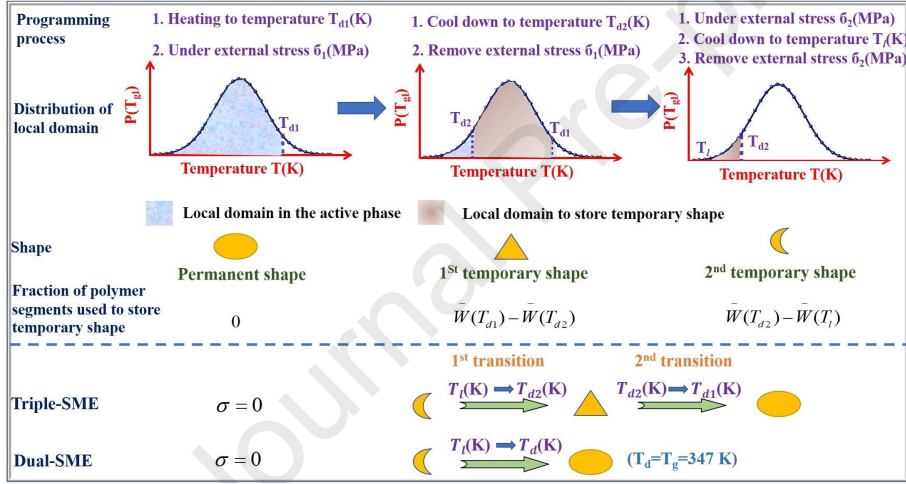


Fig. 1. Illustration of mechanical processes and their working mechanisms of SME and TME in miscible polymer blends.

According to the effect of mechanical process on SME, the phase evolution function can be expressed as follows:

$$\phi_f(T, t, T_d) = \frac{\varepsilon_s(T, t) - \varepsilon_r}{\varepsilon_{pre} - \varepsilon_r} = \begin{cases} 1 & (0 \leq \bar{W}(T, t) \leq \bar{W}(T_l)) \\ \frac{\bar{W}(T_d) - \bar{W}(T, t)}{\bar{W}(T_d) - \bar{W}(T_l)} & (\bar{W}(T_l) \leq \bar{W}(T, t) \leq \bar{W}(T_d)) \\ 0 & (\bar{W}(T_d) \leq \bar{W}(T, t) \leq 1) \end{cases} \quad (16)$$

where T_l is the initial temperature for free shape recovery of polymer.

In this paper, the proposed models are used to compare with the experimental data of the 50% PLLA/50% PMMA miscible polymer blends reported in Ref. [18], in which PLLA is the 1st blend ($T_{g1}=343$ K) and PMMA is the 2nd blend ($T_{g2}=403$ K). The glass transition widths of two components are obtained from the dynamic thermomechanical analysis (DMA) of pure PLLA and PMMA materials [29]. Universal global algorithm was then used to determine the value of parameters in equation (16). As shown in Figure 2, equation (16) was used to obtain the data of miscible PLLA/PMMA polymer with the composition of 50%:50% and the results are then compared with the experimental data reported in Ref. [18]. Values of parameters used in equation (16) during calculation are listed in table 1. With an increase in temperature from 331 K to 366.1 K at a constant heating rate of $q=1.95$ K/min, the stored strain is gradually decreased from 81.2% to 12.9%. The results obtained using the newly proposed model fit well with experimental data [18], where the glass transition temperature and deformation temperature both are 347 K.

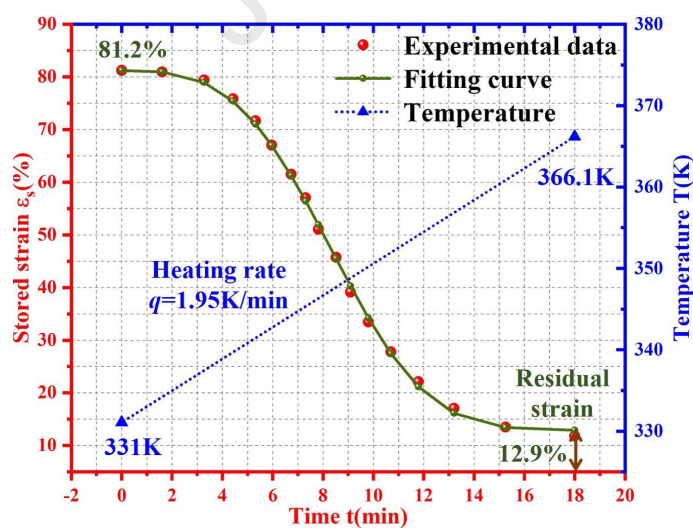


Fig. 2. Comparison between simulation results of equation (16) and experimental data [18] for miscible PLLA/PMMA polymer.

Table 1. Values of parameters used in equation (16).

T^*	T_{g1}	T_{g2}	w_1	w_2	$\Delta\mu$	ζ	ν	$B\tau_0$	β	$\bar{W}(T_d)$
773 K	343 K	410 K	63 K	77 K	3.1	200 K	4777 s ⁻¹	1357 s	3	83%

The calculation results of phase evolution fraction ($\phi_f(T, t, T_d)$) as a function of recovery time are further presented in Figure 3. Figure 3(a) shows the calculation of phase evolution function of miscible PLLA/PMMA polymer with various deformation temperatures, e.g., $T_d=330\text{K}$, 335K , 340K and 345K , and the finished transition temperatures of miscible polymers are 337K , 343K , 350K and 358K , where $\phi_f(T, t, T_d)=0$. According to equation (16), the phase evolution function $\phi_f(T, t, T_d)=0$ is for the case of $\bar{W}(T_d)-\bar{W}(T, t)=0$. Therefore, the value of $\bar{W}(T_d)$ is smaller when at a lower deformation temperature (T_d), thus resulting in the shape recovery behavior finished at a lower temperature and the recovery time decreased.

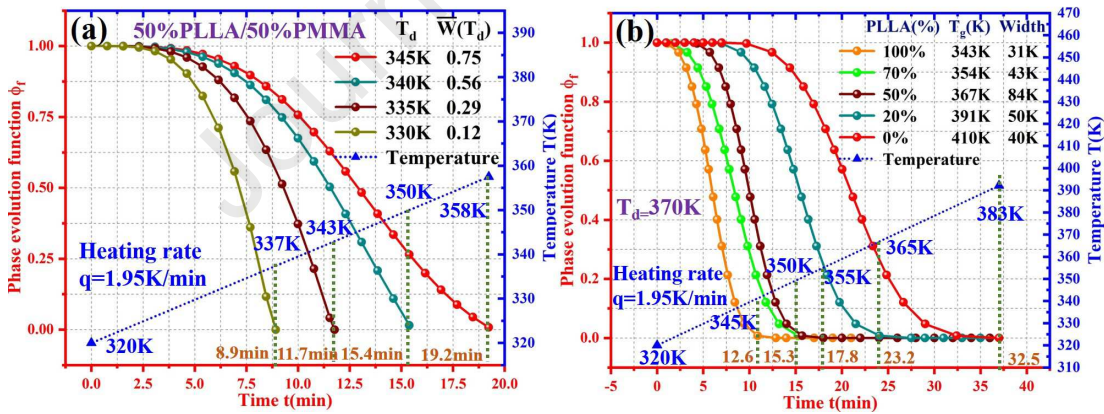


Fig. 3. Phase evolution function with respect to recovery time (a) At various deformation temperatures of $T_d=330\text{K}$, 335K , 340K and 345K ; (b) At various compositions of PLLA of $\alpha_1=0\%$, 20% , 50% , 70% and 100% .

On the other hand, effect of composition (α_1) of PLLA blend on the phase evolution fraction ($\phi_f(T, t, T_d)$) of PLLA/PMMA miscible polymer blends at a

deformation temperature of $T_d=370$ K is shown in Figure 3(b). The calculation results reveal that the glass transition temperature is gradually increased from 343 K, 354 K, 367 K, 391 K to 410 K with a decrease in composition of PLLA component from 100%, 70%, 50%, 20% to 0. Meanwhile, the corresponding widths of glass transition zones are 31 K, 43 K, 84 K, 50 K and 40 K, respectively.

Furthermore, effects of temperature and heating rate on the phase evolution function were investigated for the PLLA/PMMA miscible polymer using our proposed model. As shown in Figure 4(a), the finished temperature is gradually increased from 361 K, 382 K, 386 K, 397 K to 400 K with an increase in heating rate (q) from 1, 2, 3, 4 to 5 K/min. The working mechanism is originated from the effect of relaxation time on phase evolution function. According to the Williams-Landel-Ferry (WLF) equation [33], the increase in heating rate results in the decrease of relaxation time and increase of temperature, respectively. Therefore, the increase in heating rate results in the increase of temperature of the miscible polymer blend in order to achieve the shape recovery. As presented in equation (16), a high temperature results in a high phase evolution function, at the same deformation temperature. The finished temperature is then increased. The working mechanism can be revealed from the calculated results as shown in Figure 4(b), where the effect of recovery time on phase evolution function has been studied. It is revealed that the recovery time is gradually decreased from 17 min, 12.8 min, 10.8 min, 3.8 min to 1.9 min with an increase in finished temperature from 350 K, 360 K, 370 K, 380 K to 390 K.

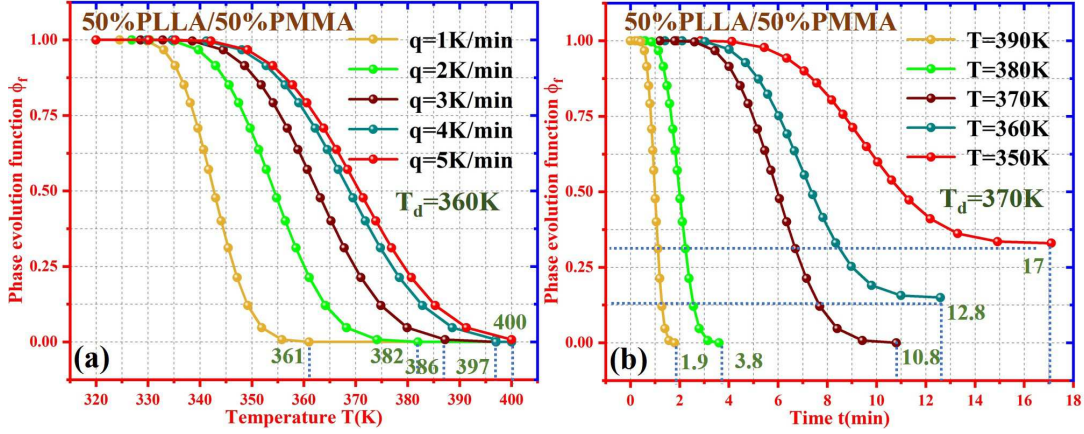


Fig. 4. (a) Phase evolution function vs. temperature, at a variety of heating rates of $q=1, 2, 3, 4$ and 5 K/min. (b) Phase evolution function vs. recovery time, at a variety of finished temperatures of $T=350, 360, 370, 380$ and 390 K.

Based on the proposed model, the effect of phase transition function on thermomechanical behavior of miscible polymers will be investigated. Here the Mori-Tanaka equation [34] is employed and the storage modulus $E_s(T, t)$ is expressed using the phase transition probability $\bar{W}(T, t)$:

$$E_s(T, t) = E_{gs} \left(1 + \frac{\bar{W}(T, t)(E_{as} / E_{gs} - 1)}{1 + \alpha(1 - \bar{W}(T, t))(E_{as} / E_{gs} - 1)} \right) \quad (17)$$

where E_{as} and E_{gs} are the storage moduli of the blend components in their active and glassy state, respectively. E_{gs} can be described using the following form [35]:

$$\log E_{gs}(T) = \log E_{gs}(T^{ref}) - \gamma(T - T^{ref}) \quad (18)$$

where $E_{gs}(T^{ref})$ is the storage modulus at reference temperature T^{ref} and γ is a parameter characterizing the temperature sensitivity of blend component.

As shown in Figure 5, the proposed model of equation (17) is used to predict the experimental results [18] of storage moduli of PLLA/PMMA miscible polymers with different compositions of 0%, 20%, 50%, 70% and 100% PLLA. Values of parameters

used in equation (17) in calculation are listed in Table 2. It is found that the calculated results from the proposed model are in good agreements with the experimental results. Meanwhile, the temperature is ranged from 330 K to 390 K and located into the glass transition temperature zone of PLLA/PMMA miscible polymer blends with 50% PLLA. Therefore, the storage modulus of PLLA/PMMA miscible polymers with 50% PLLA presents a sudden drop in Figure 5, due to the glass transition.

Table 2. Value of parameters in equation (17).

Composition of PLLA(%)	$E_{gs}(T^{ref})(\text{MPa})$	γ	$T^{ref}(\text{K})$	$E_{as}(\text{MPa})$	α
0	5011.8	0.0051	300.47	4.9	0.90
20	2818.3	0.0046	355.84		0.99
50	4073.8	7.23×10^{-9}	333.85		0.073
70	2398.8	5.43×10^{-17}	379.04		0.92
100	2818.1	5.6×10^{-4}	200.99		0.64

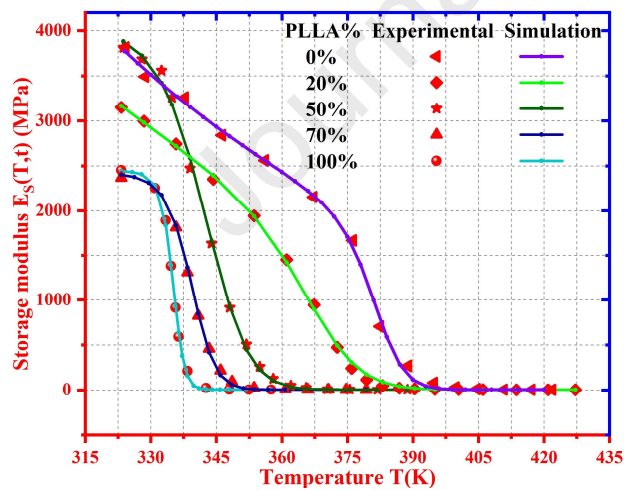


Fig. 5. Comparison between simulation results of equation (17) and experimental data [18] of the storage modulus of PLLA/PMMA miscible polymer with blend composition of 0%, 20%, 50%, 70% and 100% PLLA.

4. Model and experimental verification of multiple-SME

For the miscible polymer blends, the triple-SME can be achieved by means of two deformation temperatures (T_{d1} and T_{d2} ($T_{d1} > T_{d2}$)) to store two stored mechanical strain (ε_{pre1} and ε_{pre2}), respectively. Based on this, equation (16) is further extended as:

$$\phi_f(T, t, T_{d1}) = \frac{\varepsilon_{s1}(T, t) - \varepsilon_{r1}}{\varepsilon_{pre1} - \varepsilon_{r1}} = \begin{cases} 1 & (0 \leq \bar{W}(T, t) \leq \bar{W}(T_{d2})) \\ \frac{\bar{W}(T_{d1}) - \bar{W}(T, t)}{\bar{W}(T_{d1}) - \bar{W}(T_{d2})} & (\bar{W}(T_{d2}) \leq \bar{W}(T, t) \leq \bar{W}(T_{d1})) \\ 0 & (\bar{W}(T_{d1}) \leq \bar{W}(T, t) \leq 1) \end{cases} \quad (19)$$

$$\phi_f(T, t, T_{d2}) = \frac{\varepsilon_{s2}(T, t) - \varepsilon_{r2}}{\varepsilon_{pre2} - \varepsilon_{r2}} = \begin{cases} 1 & (0 \leq \bar{W}(T, t) \leq \bar{W}(T_1)) \\ \frac{\bar{W}(T_{d2}) - \bar{W}(T, t)}{\bar{W}(T_{d2}) - \bar{W}(T_1)} & (\bar{W}(T_1) \leq \bar{W}(T, t) \leq \bar{W}(T_{d2})) \\ 0 & (\bar{W}(T_{d2}) \leq \bar{W}(T, t) \leq 1) \end{cases} \quad (20)$$

Equations (19) and (20) were then used to calculate the stored strain of the PLLA/PMMA miscible polymer with triple-SME, and the results are compared with the experimental data reported in Ref. [18]. The deformation temperatures are $T_{d1} = 367$ K and $T_{d2} = 338$ K, and the stored mechanical strains are ε_{pre1} and ε_{pre2} , respectively. As shown in Figure 6, the stored strain of miscible polymer is initially induced from 100% to 52.4% when the temperature is increased from 303 K to 343 K. It takes 65 min to complete the full shape recovery. On the other hand, the second recovery process can be achieved when the polymer is further heated to 367 K, where the stored strain is decreased from 52.4% into 20.5%. It is found that the simulation results fit well with the experimental ones. This comparison reveals that the proposed

model is suitable to characterize and predict the triple-SME in miscible polymer.

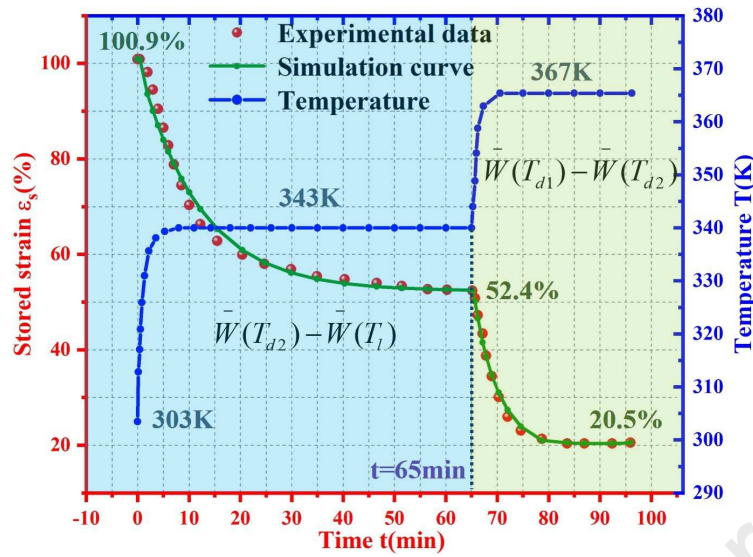


Fig. 6. Comparison of stored strain with respect to relaxation time between simulation results and experimental data [18] of miscible polymer with triple-SME.

Next, the theoretical model was used to investigate effects of macroscopic compositions on the triple-SME in miscible polymer blends. The same programming process in Figure 6 is applied to PLLA/PMMA miscible polymer blends with different content fractions of PLLA, and the heating rate (q) is kept a constant and equals to 0.5K/min. As shown in Figure 7, the triple-SME in 50%PLLA/50%PMMA miscible polymer blend is the most obvious one. With an increase in the weight fraction of PMMA in PLLA/PMMA miscible polymer blend from 60% to 80%, the distribution of local domains with different glass transition temperatures is assembled to the T_g ($T_g=390$ K) of PMMA. Since the absence of corresponding local domains response to the first temporary shape at 338K, the triple-SME in PLLA/PMMA miscible polymer blend therefore turns to be inapparent with an increase of the weight fraction of the PMMA from 60% to 80%, resulting in a dual-SME in the 20%PLLA/80%PMMA

miscible polymer blend. This simulation results reveal that the uniform distribution of local domains with different transition temperatures is significant to trigger the multi-SME of miscible polymer blends. Finally, the complete transition temperature is 370 K, which is almost equal to the deformation temperature (367K), indicating the existence of TME.

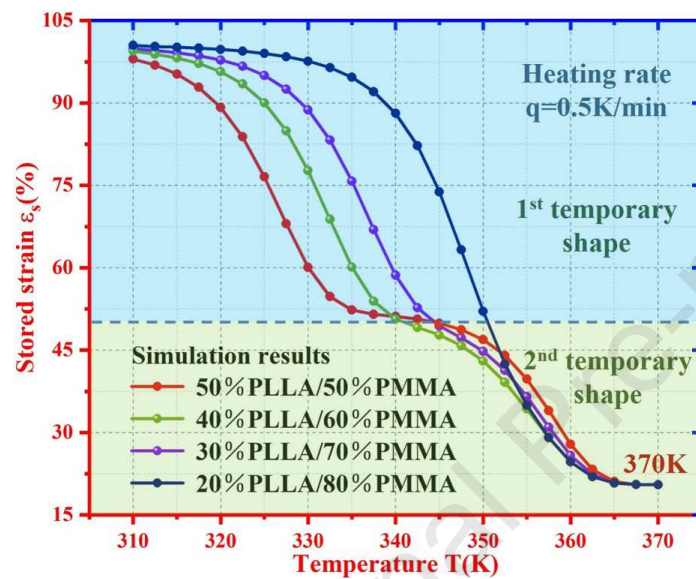


Fig. 7. Simulation results of the segmental release of the stored strain in PLLA/PMMA miscible polymer blends, with the content fraction of PLLA is 20%, 30%, 40% and 50%, respectively.

Furthermore, the proposed model is then used to characterize the quadruple-SME and quintuple-SME in miscible polymer blends. As shown in Figure 8(a), the stored strain of miscible polymer blends with a quadruple-SME has been investigated at three deformation temperatures of 340 K, 360 K and 380 K. The predicted results show that the polymer takes 67 min, 22 min and 12 min to complete the three recovery processes, respectively. On the other hand, the stored strain of miscible polymer with the quintuple-SME is further investigated as shown in Figure 8(b), where the four deformation temperatures are 340 K, 355 K, 370 K and 385 K. The

polymer takes quartic recovery processes to complete the shape recovery from $\varepsilon_s = 100\%$ to $\varepsilon_s = 0$.

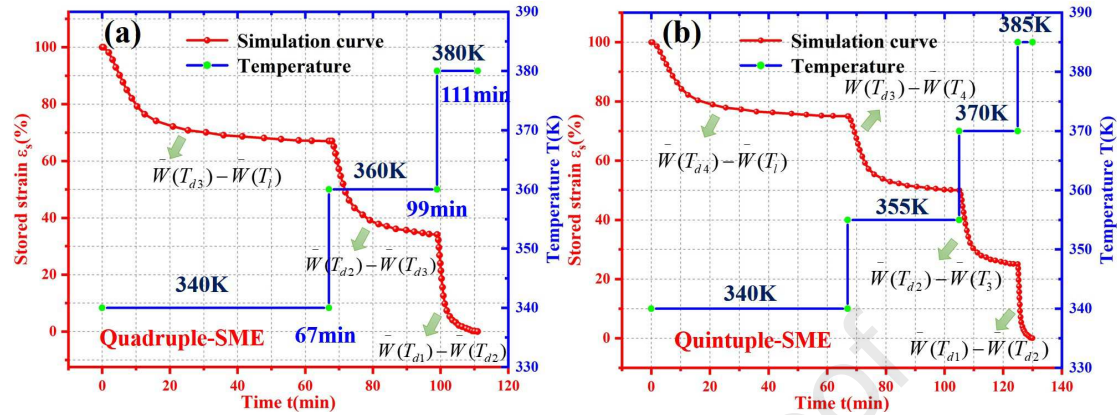


Fig. 8. (a) Simulation of stored strain as a function of relaxation time of miscible polymer blend with quadruple-SME (b) Simulation of stored strain as a function of relaxation time of miscible polymer blend with quintuple-SME.

To verify the proposed model of multi-SME, equation (16) is further used to predict the quadruple-SME of PFSA (perfluorosulphonic acid ionomer) SMPs [15], which has a broad width zone of T_g (e.g., 328 K-403 K), as shown in Figure 9. Values of parameters used in equation (16) during calculation are listed in table 3. The stored strain of PFSA SMP with a quadruple-SME has been investigated at different deformation temperatures of 326 K, 363 K and 413 K. At a constant heating rate, the first shape transition of SMP is induced in temperature from 293 K to 326 K. And the temporary shape is kept at 326 K. Consequently, the second shape transition of SMP is further induced with an increase in temperature from 326 K to 363 K, and the third shape transition is achieved by increasing temperature from 363 K to 413 K. Therefore, a quadruple SME has been achieved for the PFSA SMP. Three domains are used to characterize the recovery behavior at each deformation temperature, and the analytical results reveal that the PFSA SMP takes 28.1 min, 27.6 min and 24.4 min to

complete the recovery processes, respectively.

Table 3. Values of parameters used in equation (16) for the PFSA SMP with quadruple-SME.

Composition	$\varepsilon_s(\%)$	$T_{0i}(K)$	$v(/s)$	$\Delta\mu(KJ/mol)$	$\varepsilon_r(\%)$
1 st temporary shape	21.5	301.4	21.6	9968.2	1.9
2 nd temporary shape	36.5	252.5	87.1		
3 rd temporary shape	60	225.1	823		

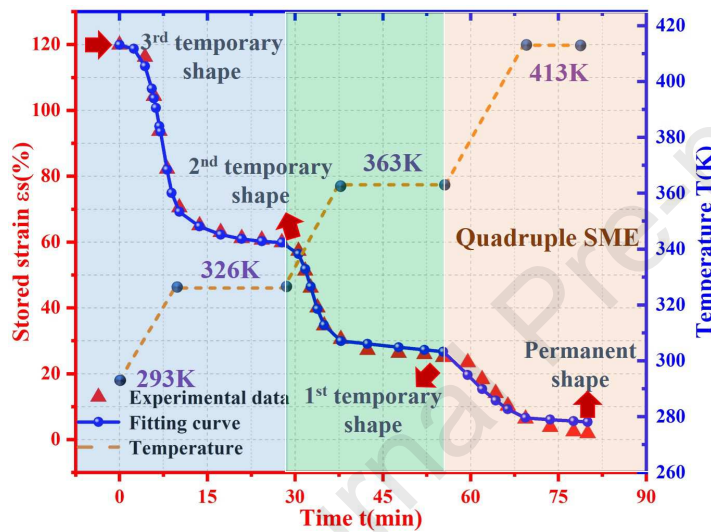


Fig. 9. Comparison of stored strain with respect to relaxation time between analytical results and experimental data [15] of PFSA SMP with quadruple-SME.

Finally, the proposed model is used to characterize and predict the mechanical behavior of the miscible polymer blends, e.g., for programming their shape deformation and free shape recovery behavior. As presented in previous studies [18], multiple-SME in miscible polymers can be designed and achieved by a variety of deformation temperatures.

To model the relaxation behavior, the Young's modulus of miscible polymer in active state ($E_{ay}(T, t)$) could be obtained using the extended Maxwell equation

[36,37]:

$$E_{ay}(T, t) = E_0 + E_1 \exp\left(-\frac{t}{\tau(T)}\right)^\beta \quad (21)$$

where E_0 is the Young's modulus of the elastic spring, and E_1 is the Young's modulus of the viscoelastic element. In combination of equations (4) and (21), the Young's modulus at active state ($E_{ay}(T, t)$) can be rewritten as:

$$E_{ay}(T, t) = E_0 + E_1 \exp\left\{-t / \left[\tau_0 \exp\left(\frac{\Delta\mu(T^* - T_0)}{RT^*(T - T_0)}\right)\right]\right\}^\beta \quad (22)$$

In combination of equations (19) and (22), the Young's modulus ($E_y(T, t)$) of miscible polymer is obtained as a function of relaxation time and temperature:

$$E_y(T, t) = E_{fs} \left(1 + \frac{\bar{W}(T, t)(E_{ay}(T, t) / E_{fy}(T) - 1)}{1 + \alpha(1 - \bar{W}(T, t))(E_{ay}(T, t) / E_{fy}(T) - 1)} \right) \quad (23)$$

According to equation (23), the deformation strain (\mathcal{E}_d) can be expressed when the polymer is under a constant external force (σ):

$$\mathcal{E}_d(T, t) = \frac{\sigma}{E_y(T, t)} = \sigma / \left\{ E_{fs} \left(1 + \frac{\bar{W}(T, t)(E_{ay}(T, t) / E_{fy}(T) - 1)}{1 + \alpha(1 - \bar{W}(T, t))(E_{ay}(T, t) / E_{fy}(T) - 1)} \right) \right\} \quad (24)$$

When the polymer is deformed at temperatures of T_{d1} to T_{d2} , the stored strain \mathcal{E}_{pre1} and \mathcal{E}_{pre2} are expressed as following, respectively,:

$$\mathcal{E}_{pre1} = \mathcal{E}_d \Big|_{T=T_{d1}} \left(\frac{\bar{W}(T_{d1}) - \bar{W}(T_{d2})}{\bar{W}(T_{d1})} \right) \quad (25)$$

$$\mathcal{E}_{pre2} = \mathcal{E}_d \Big|_{T=T_{d2}} \left(\frac{\bar{W}(T_{d2}) - \bar{W}(T_{d1})}{\bar{W}(T_{d2})} \right) \quad (26)$$

The mechanical history and relaxation behavior of miscible polymer blends, which has dual-SME (under a deformation stress of 0.69 MPa) and triple-SME (under the

deformation stresses of 0.1 MPa and 2.0 MPa), have been plotted in Figure 10. Experimental data reported in Ref. [18] of miscible PLLA/PMMA polymer with dual- and triple-SMEs have been employed to verify the results predicted using the proposed models, e.g., equations (24), (25) and (26). As revealed in Figure 10(a), the miscible polymer blends undergo a deformation at 347 K and has a stored strain of 81.2%. In the free recovery process, the stored strain of polymer is decreased from 81.2% to 12.9% with an increase in temperature from 280 K to 366.1 K. It is found that results from the proposed models are in good agreement with the experimental data. Furthermore, the polymer reveals a glass transition temperature of 347 K and it is equal to the deformation temperature. Therefore, the TME is also achieved by the proposed models, as $T_g = T_d$.

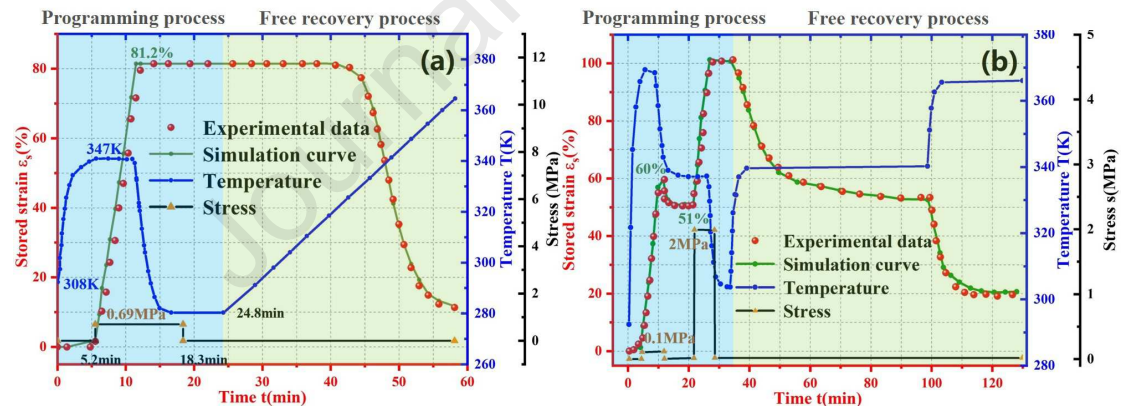


Fig. 10. Comparison between equations (24), (25) and (26), and the experimental data [18] of both the programming process and the recovery process of miscible PLLA/PMMA polymer. (a) For dual-SME; (b) For triple-SME.

On the other hand, the triple-SME in miscible polymer was further investigated and the predicted results using the model are shown in Figure 10(b). Here, the polymer undergoes a first deformation at an external stress of 0.1 MPa and achieves 60%

stored strain. Then the stress is released and the polymer is cooled back from 370 K to 340 K, resulting in a stored strain of 51% remained in polymer. Furthermore, an external stress of 2.0 MPa was applied and the polymer is cooled back to 308 K from 340 K to achieve a 100% stored strain. Therefore, the miscible polymer blend undergoes the first relaxation behavior when it is heated from 308 K to 340 K and then the second behavior at the temperature is ranged from 340 K to 370 K. The stored strain is gradually decreased from 100% to 52.4% and from 52.4% to 20.5% in the first and second relaxation processes, respectively. These simulation results reveal that the proposed models can well fit and predict the mechanical history and relaxation behavior for the miscible polymer blends, with both dual-SME and triple-SME. The same working mechanisms of dual-SME and triple-SME can be then extended to the multiple-SME in the miscible polymer blend.

5. Conclusions

In this study, a thermodynamic domain size model was formulated to understand the SME working mechanism from the perspective of unique dynamic coordination between different phases in the miscible polymer. The combination of AG theory and coupling model was initially used to investigate the effect of component heterogeneities on dynamic conformational entropy, glass transition and relaxation behaviours of miscible polymer blend. Effects of component heterogeneities on dynamic conformational entropy, glass transition and relaxation behaviours of miscible polymer blend were systematically studied. Both the SME and TME in miscible polymer blends have been

well-described using our newly proposed model. Finally, the model was applied to predict dual- and triple-SME in SMPs, respectively, and the theoretical results are validated by the experiments. We expect this approach to shed the light in the design and development of future miscible polymer blends with versatile SME for frontier engineering applications.

Declaration of competing interest

The authors declare that they have no known competing financial interests or personal relationships that could have appeared to influence the work reported in this paper.

Acknowledgements

This work was financially supported by the National Natural Science Foundation of China (NSFC) under Grant No. 11672342 and 11725208, Newton Mobility Grant (IE161019) through Royal Society and NFSC.

References

- [1] R. Hoehner, T. Raidt, F. Katzenberg, J.C. Tiller, Heating rate sensitive multi-shape memory polypropylene: a predictive material, *ACS Appl. Mater. Inter.* 8 (22) (2016) 13684–13687.
- [2] H.B. Lu, J.S. Leng, S.Y. Du, A phenomenological approach for the chemo-responsive shape memory effect in amorphous polymers, *Soft Matter* 9 (14) (2013) 3851–3858.
- [3] H. Zhang, Y. Zhao, Polymers with dual light-triggered functions of shape memory and healing using gold nanoparticles, *ACS Appl. Mater. Inter.* 5 (24) (2013) 13069–13075.
- [4] B. Xu, L. Zhang, Y.T. Pei, J.K. Luo, S.W. Tao, J.T.M. De Hosson, Y.Q. Fu, Electro-responsive polystyrene shape memory polymer nanocomposites, *Nanosci. Nanotech. Lett.* 4 (8) (2012) 814–820.
- [5] X. Wang, W. Jian, H. Lu, D. Lau, Y.Q. Fu, Modeling Strategy for Enhanced Recovery Strength and a Tailorable Shape Transition Behavior in Shape Memory Copolymers, *Macromolecules.* 52 (16) (2019) 6045–6054.
- [6] V.C. Sonawane, M.P. More, A.P. Pandey, P.O. Patil, P.K. Deshmukh, Fabrication and characterization of shape memory polymers based bioabsorbable biomedical drug eluting stent *Artif. Cells, Nanomedicine Biotechnol.* 45 (8) (2017) 1740–1750.
- [7] Y. Guo, Z. Lv, Y. Huo, L. Sun, S. Chen, Z. Liu, C. He, X. Bi, X. Fan, Z. You A biodegradable functional water-responsive shape memory polymer for biomedical applications, *J. Mater. Chem. B* 7 (1) (2019) 123–132.
- [8] R. Tao, Q. Yang, X. He, K. Liew, Parametric analysis and temperature effect of deployable hinged shells using shape memory polymers, *Smart. Mater. Struct.* 25 (11) (2016) 115034.
- [9] M.J., Jo, H. Choi, G.H. Kim, W.R. Yu, M. Park, Y. Kim, J.K. Park, J.H. Youk, Preparation of epoxy shape memory polymers for deployable space structures using flexible diamines fibers, *Polymer* 19 (9) (2018) 1799–1805.

- [10] H.B. Lu, M. Lei, C. Zhao, B. Xu, J.S. Leng, Y.Q. Fu, Structural design of flexible Au electrode to enable shape memory polymer for electrical actuation, *Smart Mater. Struct.* 24 (4) (2015), 045015.
- [11] F. Pilate, A. Toncheva, P. Dubois, J.M. Raquez, Shape-memory polymers for multiple applications in the materials world, *Eur. Polym. J.* 80 (2016) 268–294.
- [12] C. Véchambre, A. Buléon, L. Chaunier, C. Gauthier, D. Lourdin, Understanding the mechanisms involved in shape memory starch: Macromolecular orientation, stress recovery and molecular mobility, *Macromolecules* 44 (23) (2011) 9384–9389.
- [13] M. Behl, I. Bellin, S. Kelch, W. Wagermaier, A. Lendlein, One-step process for creating triple-shape capability of AB polymer networks, *Adv. Funct. Mater.* 19 (1) (2009) 102–108.
- [14] I. Bellin, S. Kelch, A. Lendlein, Dual-shape properties of triple-shape polymer networks with crystallizable network segments and grafted side chains, *J. Mater. Chem.* 17 (28) (2007) 2885–2891.
- [15] T. Xie, Tunable polymer multi-shape memory effect, *Nature* 464 (7286) (2010) 267–270.
- [16] J. Li, T. Xie, Significant impact of thermo-mechanical conditions on polymer triple-shape memory effect, *Macromolecules* 44 (1) (2011) 175–180.
- [17] L. Sun, W.M. Huang, Mechanisms of the multi-shape memory effect and temperature memory effect in shape memory polymers, *Soft Matter* 6 (18) (2010) 4403–4406.
- [18] C. Samuel, S. Barrau, J.M. Lefebvre, J.M. Raquez, P. Dubois, Designing multiple-shape memory polymers with miscible polymer blends: Evidence and origins of a triple-shape memory effect for miscible PLLA/PMMA blends, *Macromolecules* 47 (19) (2014) 6791–6803.
- [19] H.M. Jeong, J.H. Song, S.Y. Lee, B.K. Kim, Miscibility and shape memory property of poly(vinyl chloride)/thermoplastic polyurethane blends, *J. Mater. Sci.* 36 (22) (2001) 5457–5463.
- [20] H.M. Jeong, B.K. Ahn, B.K. Kim, Miscibility and shape memory effect of

- thermoplastic polyurethane blends with phenoxy resin, *Eur. Polym. J.* 37 (11) (2001) 2245–2252.
- [21] B. Xu, Y.Q. Fu, W.M. Huang, Y.T. Pei, Z.G. Chen, J.T.M. De Hosson, A. Kraft, R.L. Reuben, Thermal-mechanical properties of polyurethane-clay shape memory polymer nanocomposites, *Polymers* 2 (2) (2010), 31–39.
- [22] M. Lei, B. Xu, Y.T. Pei, H.B. Lu, Y.Q. Fu, Micro-mechanics of nanostructured carbon/shape memory polymer hybrid thin film, *Soft Matter* 12 (1) (2016) 106–114.
- [23] Q. Yang, G. Li, Temperature and rate dependent thermomechanical modeling of shape memory polymers with physics based phase evolution law, *Int. J. Plast.* 80 (2016) 168–186.
- [24] K. Yu, T. Xie, J. Leng, Y. Ding, H.J. Qi, Mechanisms of multi-shape memory effects and associated energy release in shape memory polymers, *Soft Matter* 8 (20) (2012) 5687–5695.
- [25] T.D. Nguyen, C.M. Yakacki, P.D. Brahmbhatt, M.L. Chambers, Modeling the relaxation mechanisms of amorphous shape memory polymers, *Adv. Mater.* 22 (31) (2010) 3411–3423.
- [26] T.D. Nguyen, J.H. Qi, F. Castro, K.N. Long, A thermoviscoelastic model for amorphous shape memory polymers: Incorporating structural and stress relaxation, *J. Mech. Phys. Solids* 56 (9) (2008) 2792–2814.
- [27] G. Adam, J.H. Gibbs, On the temperature dependence of cooperative relaxation properties in glass-forming liquids, *J. Chem. Phys.* 43 (1) (1965) 139–146.
- [28] S. Matsuoka, Entropy, free volume, and cooperative relaxation, *J. Res. Natl. Inst. Stand. Technol.* 102 (2) (1997) 213-219.
- [29] P. Shi, R. Schach, E. Munch, H. Montes, F. Lequeux, Glass transition distribution in miscible polymer blends: From calorimetry to rheology, *Macromolecules* 46 (9) (2013) 3611–3620.
- [30] K.L. Ngai, Modification of the Adam-Gibbs model of glass transition for consistency with experimental data, *J. Phys. Chem. B* 103 (28) (1999) 5895–5902.

- [31] P.K. Gupta, J.C. Mauro, The laboratory glass transition, *J. Chem. Phys.* 126 (22) (2007) 224504.
- [32] S. Matsuoka, X. Quan, Intermolecular cooperativity in dielectric and viscoelastic relaxation, *J. Non. Cryst. Solids* 131 (1) (1991) 293–301.
- [33] M.L. Williams, R.F. Landel, J.D. Ferry, The temperature dependence of relaxation mechanisms in amorphous polymers and other glass-forming liquids, *J. Am. Chem. Soc.* 77 (14) (1955) 3701–3707.
- [34] P. Gilormini, J. Diani, On modeling shape memory polymers as thermoelastic two-phase composite materials, *CR. Mecanique* 340 (4-5) (2012) 338–348.
- [35] J. Richeton, G. Schlatter, K.S. Vecchio, Y. Rémond, S. Ahzi, A unified model for stiffness modulus of amorphous polymers across transition temperatures and strain rates, *Polymer* 46 (19) (2005) 8194–8201.
- [36] D. Zhong, Y. Xiang, T. Yin, H. Yu, S. Qu, W. Yang, A physically-based damage model for soft elastomeric materials with anisotropic Mullins effect, *Int. J. Solids Struct.* 176–177 (2019) 121–134.
- [37] Q. Ge, K. Yu, Y. Ding, J.H. Qi, Prediction of temperature-dependent free recovery behaviors of amorphous shape memory polymers, *Soft Matter* 8 (43) (2012) 11098–11105.

Highlights:

- The thermodynamics of shape memory effect (SME) in miscible polymer blends has been explored
- An approach of highly designable SMEs with adjustable glass transition temperature and width of glass transition zone
- An extended domain size model was formulated based on the Adam-Gibbs theory and Gaussian distribution theory

Journal Pre-proof

Declaration of interests

The authors declare that they have no known competing financial interests or personal relationships that could have appeared to influence the work reported in this paper.

The authors declare the following financial interests/personal relationships which may be considered as potential competing interests:

Journal Pre-proof